

# Unusual Hall Effect Anomaly in MnSi Under Pressure

Minhyea Lee<sup>1†</sup>, W. Kang<sup>2</sup>, Y. Onose<sup>3</sup> Y. Tokura<sup>3,4</sup> and N. P. Ong<sup>1</sup>

<sup>1</sup>*Department of Physics, Princeton University, Princeton, NJ 08544, USA*

<sup>2</sup>*Department of Physics, University of Chicago, Chicago, IL 60637, USA*

<sup>3</sup>*Department of Applied Physics, University of Tokyo,*

*Tokyo 113-8656, Japan* <sup>4</sup>*ERATO, JST,*

*Spin Superstruture Project (SSS), Tsukuba 305-8562, Japan*

(Dated: May 5, 2009)

## Abstract

We report the observation of a highly unusual Hall current in the helical magnet MnSi in an applied pressure  $P = 6\text{--}12$  kbars. The Hall conductivity displays a distinctive step-wise field profile quite unlike any other Hall response observed in solids. We identify the origin of this Hall current with the effective real-space magnetic field due to chiral spin textures, which may be a precursor of the partial-order state at  $P > 14.6$  kbar. We discuss evidence favouring the chiral spin mechanism for the origin of the observed Hall anomaly.

PACS numbers: 72.15.Gd, 72.25.Ba, 75.30.Kz, 75.45.+j

In the helical, itinerant magnet MnSi, a novel magnetic state with “partial order” has been reported by Pfleiderer and coworkers above a critical applied pressure  $P_c = 14.6$  kbar [1, 2, 3]. The neutron diffraction intensity is broadly distributed over the surface of a sphere in momentum space, but is resolution limited in the radial direction. Several groups have proposed that the state harbors non-trivial topological spin textures [4, 5, 6, 7]. We have observed a highly unusual Hall current in MnSi at pressures (6–12 kbar) just below  $P_c$ , which appears to be caused by fluctuations into the chiral spin state at temperatures  $T$  near the Curie transition temperature  $T_C$ .

At ambient pressure, MnSi, which is non-centrosymmetric with the crystal structure B20, undergoes a transition at  $T_C \simeq 30$  K to a helical state with a long pitch  $\lambda \sim 180$  Å. The wavevector  $\mathbf{q}$  is weakly pinned along the  $\langle 111 \rangle$  direction. The helical state reflects the competition between the exchange energy and the Dzyaloshinsky-Moriya term [8, 9, 10]. In a magnetic field  $\mathbf{H}$ ,  $\mathbf{q}$  shifts to alignment, and the helical state evolves to a conical magnetic state, whose cone angle steadily decreases to zero at a field  $H_s \sim 0.6$  T. Under pressure,  $T_C$  decreases monotonically, reaching zero at the critical pressure  $P_c \sim 14.6$  kbar (Fig. 1, inset). Above  $P_c$ , the “partial-order” state displays a non-Fermi liquid exponent in its resistivity [1] in addition to the unusual neutron diffraction spectrum.

The new Hall anomaly is observed in weak  $H$  in the pressure interval  $6 < P < 12$  kbar below the curve of  $T_c$  vs.  $P$  (shaded region in the inset of Fig. 1). Figure 1 (main panel) displays the Hall resistivity  $\rho_{yx}$  measured at several temperatures ( $T$ ) with  $P$  fixed at 11.4 kbar ( $T_C = 11.3$  K). At the lowest  $T$  (0.35 and 2.5 K),  $\rho_{yx}$  is hole-like and  $H$ -linear. Between 5 and 10 K, however, we observe a prominent Hall anomaly with a most unusual profile. The step-like onset at the field  $H_1 \sim 0.1$  T and the equally abrupt disappearance at  $H_2 \sim 0.45$  T stands in sharp contrast with the broad background at higher  $H$  [the latter is the *conventional* anomalous Hall effect (AHE) term common to all ferromagnets]. We show below that this unusual anomaly is the Hall-current response produced by coupling between the spin of charge carriers with chiral spin textures. Its observation provides strong evidence that the chiral spin textures exist over a large fraction of the phase diagram for  $P < P_c$ .

Motivated by the results of Refs. [1, 2, 3], several groups [4, 5, 6, 7] have proposed states comprised of crystalline arrays of magnetic textures. In Ref. [7], the transition at  $P_c$  is from a single-spiral state to a bcc “spin crystal” comprised of 6 spirals. In Refs. [4, 5], the proposed state is either a square lattice configuration of topological defects called skyrmions [4, 5],

or a cubic network of line defects which are double-twist configurations [5]. The textures are closely related to the defects previously studied in the blue phase of nematic liquid crystals [5, 6].

Hall measurements were made in a  $^3\text{He}$  cryostat using a miniature clamp-type pressure cell (13 mm dia.) made of BeCu alloy and tungsten carbide with Fluorinert (FC-77) as the pressure medium. At low  $T$ , the pressure was calibrated by the superconducting transition of a Pb coil detected by AC susceptibility. The high-purity MnSi crystals (of resistivity ratio  $\rho(300\text{K})/\rho(4.2\text{K}) \simeq 60$  and size  $1.1 \times 0.5 \times 0.060 \text{ mm}^3$ ) were cut from boules grown in a floating-zone furnace. The Hall voltage  $V_H$  was checked to scale linearly with current  $I$  (typically 0.5 to 1 mA). At each  $T$  and  $P$ ,  $V_H$  was recorded with  $H$  swept at the rate 0.02 T/min. in the sequence  $0 \rightarrow -1T \rightarrow 0 \rightarrow 1T \rightarrow 0$  to eliminate errors from induced emf's and drifts in  $T$ . The observed Hall anomaly is always antisymmetric in  $H$  even without antisymmetrization of the 4 raw curves. Results obtained in the 2 crystals investigated are closely similar.

In ferromagnets, the observed Hall resistivity  $\rho_{yx}$  is the sum of the ordinary Hall resistivity  $\rho_{yx}^N = \sigma_{xy}^N \rho^2$  and the AHE term  $\rho_{yx}^A = \sigma_{xy}^A \rho^2$ , where  $\rho = \rho_{xx}$  is the resistivity and  $\sigma_{xy}^N$  and  $\sigma_{xy}^A$  are the ordinary and anomalous Hall conductivities, respectively. Dividing by  $\rho^2$ , we have

$$\frac{\rho_{yx}}{\rho^2} = \sigma_{xy}^N + \sigma_{xy}^A. \quad (1)$$

The first term is strictly  $H$  linear in low  $H$ , while the second term scales as the uniform magnetization  $M(T, H)$ .

To bring out the surprising nature of the new anomaly, we recall the salient features of the Hall Effect at ambient  $P$  [11, 12]. In high-purity MnSi, Lee *et al.* [12] have shown that, in spite of the large magnetoresistance (MR), the  $H$  dependence of  $\sigma_{xy}^A$  at ambient  $P$  strictly mimics that of  $M(T, H)$ , viz.  $\sigma_{xy}^A(T, H) = S_H M(T, H)$ , with  $S_H$  a constant independent of  $T$  and  $H$ . This scaling confirms a key prediction of the Karplus-Luttinger (KL) theory [13] (and its generalization using the Berry phase [14, 15, 16]).

Returning to the Hall curves in MnSi under pressure, we plot in Fig. 2 curves of  $\rho_{yx}$  over a broader field range, with  $P$  fixed at 8.5 kbar (at which  $T_C = 16.4 \text{ K}$ ). Starting at 5 K, we observe that  $\rho_{yx}$  is linear in  $H$  to 7 T. This reflects the dominance of  $\sigma_{xy}^N \sim \ell^2$  in the limit of large mean-free-path  $\ell$ . With increasing  $T$ , however, the rapid increase of  $\rho$  strongly amplifies the anomalous term  $\rho_{yx}^A$  which emerges as a negative contribution with a broad

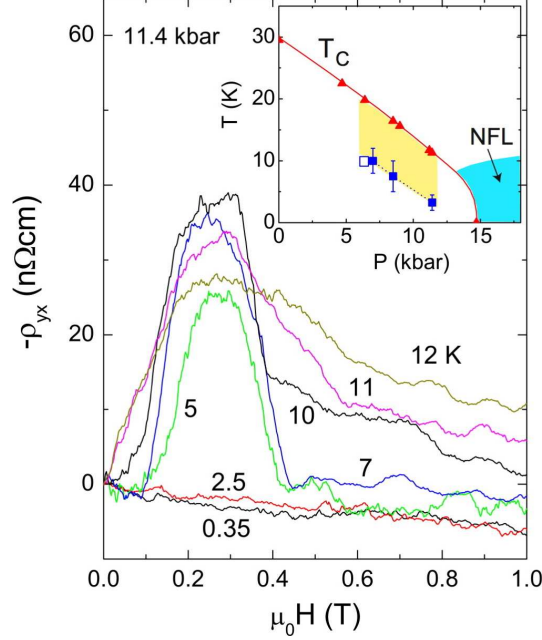


FIG. 1: (color online) (Main panel) Curves of  $-\rho_{yx}$  in MnSi at 11.4 kbar revealing a large Hall anomaly in the field range  $0.1 < H < 0.45$  T for several  $T < T_C$  ( $T_C = 11.3$  K), with  $\mathbf{H}$  nominally along (111). The anomaly (electron-like in sign) arises from a new contribution  $\sigma_{xy}^C$  to the total Hall conductivity. In the phase diagram (inset), the shaded region is where  $\sigma_{xy}^C$  is resolved.  $T_C$  was determined from  $\rho$  vs.  $T$ . Data from Samples 1 and 2 are shown as solid and open squares, respectively. The non-Fermi liquid (NFL) region is shaded blue (adapted from Ref. [2]).

shoulder (e.g. at 2.5 T at 25 K). We refer to this term as the “conventional” AHE term. At 10 and 15 K, we see the emergence of the new Hall anomaly as a sharp negative spike in weak fields. Raising  $T$  above  $T_C$  removes the spike (curves at 20 and 25 K). The curves above  $T_C$  are closely similar to those observed at ambient  $P$  (where the spike is absent).

The new Hall anomaly is qualitatively distinct from the Lorentz-force term and the KL term. As mentioned, theory predicts that coupling of the carrier spin to local textures of  $\mathbf{M}(\mathbf{r})$  produces a large anomalous Hall current via the Berry phase [17, 18]. In the past decade, the Berry-phase approach has greatly extended the purview of the KL theory [14, 15, 16]. In a periodic lattice, the “overlap” of wave functions  $u_{\mathbf{k}}$  defines the Berry gauge potential  $\mathbf{A}(\mathbf{k}) = \langle u_{\mathbf{k}} | i \nabla_{\mathbf{k}} | u_{\mathbf{k}} \rangle$ , whose curl gives an effective magnetic field  $\mathbf{\Omega}(\mathbf{k})$  that lives in  $\mathbf{k}$  space. When  $\mathbf{\Omega}(\mathbf{k})$  is rendered finite (by breaking time-reversal invariance), it leads to orbit deflection in  $\mathbf{k}$  space, to reproduce the KL term  $\sigma_{xy}^A$  in Eq. 1.

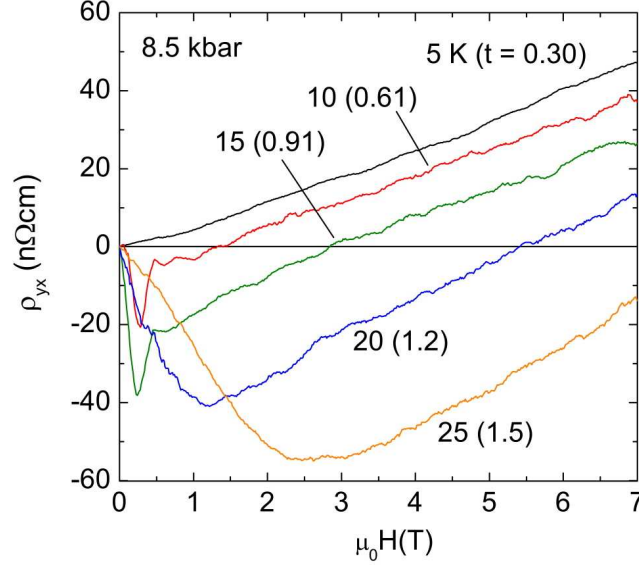


FIG. 2: (color online) Curves of  $\rho_{yx}$  extending to 7 T showing the relation of the Hall anomaly to other Hall terms (at the applied  $P = 8.5$  kbar,  $T_C = 16.4$  K). At 5 K, the hole-like  $\sigma_{xy}^N$  dominates  $\rho_{yx}$  to produce an  $H$ -linear background. At  $T = 10$  and 15 K, at which the Hall anomaly is observed as sharp negative spikes, the AHC term  $\rho_{yx}^A = \sigma_{xy}^A \rho^2$  grows in prominence as  $\rho$  increases. Above  $T_C$  (20 and 25 K), the Hall anomaly vanishes, while  $\rho_{yx}^A$  continues to increase in magnitude. The reduced temperature  $t = T/T_C$  is shown in parenthesis for each curve.

Quite distinct from this strictly orbital coupling, the Berry phase can produce an *additional* effective magnetic field  $\mathbf{B}_\phi$  via the spin degrees of freedom. The spin-mediated mechanism was initially invoked to explain AHE experiments in manganites [19] and pyrochlores [20]. We consider the simplest example in which the spin  $\mathbf{s}$  of a hopping electron aligns by Hund coupling  $J_H$  to the ion's local moment  $\mathbf{S}_i$  at each site  $i$  [19, 20]. As the electron completes a closed loop linking 3 non-coplanar spins  $\mathbf{S}_i$  ( $i = 1, 2, 3$ ),  $\mathbf{s}$  describes a cone of finite solid angle  $\Omega_s$  (Fig. 3, inset). Hence, the electron acquires a Berry phase  $\phi_B = \frac{1}{2}\Omega_s$ , which translates to a magnetic field in real space  $B_\phi = (\phi_B/2\pi)(\phi_0/\mathcal{A})$  that can be extremely large ( $\mathcal{A}$  is the loop area and  $\phi_0$  the flux quantum). For e.g., even for  $\Omega_s \sim \pi/100$  over an area  $\mathcal{A} \sim 5 \times 5 \text{ \AA}^2$ , we have  $B_\phi \sim 42$  T. In turn,  $\mathbf{B}_\phi$  produces a large Hall conductivity  $\sigma_H^C$  that is proportional to the chirality  $\chi_c = \mathbf{S}_1 \cdot \mathbf{S}_2 \times \mathbf{S}_3$  [17, 18, 20].

The foregoing also applies to itinerant ferromagnets [18]. In a spiral helimagnet such as MnSi, the local spin direction  $\mathbf{S}(\mathbf{r})$  varies periodically with a pitch set by the wavevector  $\mathbf{q}$ . For an itinerant electron, the exchange energy forces its spin  $\mathbf{s}$  to follow the spatial variation

of  $\mathbf{S}(\mathbf{r})$ . However, as emphasized in Ref. [21], a spiral state with a single  $\mathbf{q}$  has zero chirality. In order to produce finite chirality, we must have a multi- $\mathbf{q}$  spiral state, as has been proposed for the partial order state for  $P > P_c$ .

In the novel states proposed [4, 5, 6, 7], the presence of skyrmions or double-twist configurations naturally leads to chirality. We expect  $\sigma_H^C$  to be proportional to the skyrmion number  $N_s = \int d^3r \Phi_z(\mathbf{r})$ , with the skyrmion density  $\Phi_z = (8\pi)^{-1} \hat{\mathbf{n}} \cdot (\partial_x \hat{\mathbf{n}} \times \partial_y \hat{\mathbf{n}})$  and  $\hat{\mathbf{n}} = \mathbf{S}(\mathbf{r})/|\mathbf{S}(\mathbf{r})|$ .

For the region of our Hall experiment ( $P < P_c$ ), we expect fluctuations towards the multi- $\mathbf{q}$  state to be favorable at temperatures just below  $T_C$  (the fluctuations are strongly suppressed as  $T \rightarrow 0$ ). Hence, within the broad swath in which  $\sigma_{xy}^C$  is observed (Fig. 1 inset), we propose that chirality exists caused by strong fluctuations into multi- $\mathbf{q}$  helical states.

There is considerable evidence for strong fluctuations in the region  $P < P_c$ . The muon spin rotation data by Uemura *et al.* [22] show that, for  $P < P_c$ , magnetic order exists only in a partial volume fraction, in agreement with conclusions from nuclear magnetic resonance [23] and neutron scattering [24] experiments. In a broad range of  $P$  below  $P_c$ , strong fluctuations appear as a precursor to the partial-ordered state above  $P_c$ .

Within this picture, we may understand several puzzling features of the Hall data (as well as the MR). To examine these issues in more detail, we transform  $\rho_{yx}$  to  $\sigma_{xy} = \rho_{yx}/\rho^2$  using the simultaneously measured curve of  $\rho$  vs.  $H$ . As plotted in Fig. 3a, the Hall anomaly is now apparent as a large Hall conductivity  $\sigma_{xy}^C$ , with a distinctive field profile. Just below  $T_C$ , the anomaly first appears as a shallow hull feature (compare curves at 12 and 11 K). With decreasing  $T$ , it deepens considerably. Comparing the curves of  $\sigma_{xy}$  with the MR curves, we see that  $\sigma_{xy}^C$  is restricted to the narrow interval  $H_1 < H < H_2$ . At 5 K, its magnitude is  $\sim 10$  times larger than the other 2 Hall terms, and  $\sim 1\%$  of the zero- $H$  conductivity  $\sigma$ . Finally, at 2.5 K, the anomaly vanishes, leaving an  $H$ -linear background that is dominated by  $\sigma_{xy}^N$ .

We next discuss the evidence for the chiral-spin mechanism. First, we note that, between  $H_1$  and  $H_2$ ,  $|\sigma_{xy}^C|$  attains remarkably large values. At ambient pressure 5 K with  $H = 0.3$  T, the measured values of the ordinary term and the KL term,  $\sigma_{xy}^N$  and  $\sigma_{xy}^A$ , are  $\sim +3.2 \times 10^4$  and  $-1.2 \times 10^4$  ( $\Omega_s \text{m})^{-1}$ , respectively [12]. By comparison,  $|\sigma_{xy}^C|$  is 10 times larger than either of these values. Such a large  $\sigma_{xy}^N$  is difficult to understand with orbital mechanisms given the small values of  $H_1$  and  $H_2$ . By contrast, the chiral spin term is easily capable of producing such a large Hall response. The effective field  $B_\phi$  can exceed 40 T despite the

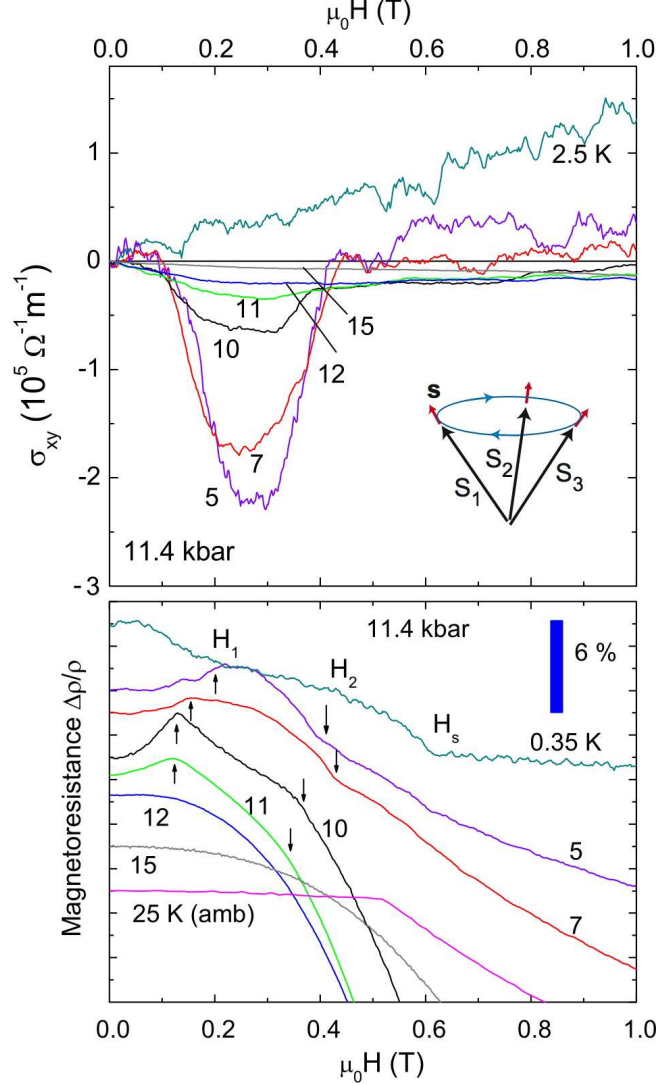


FIG. 3: (color online) Panel (a) Curves of  $\sigma_{xy}$  vs.  $H$  at  $P = 11.4$  kbar at selected  $T$ . The Hall anomaly  $\sigma_{xy}^C$  is prominent between 11 and 5 K between the fields  $H_1$  and  $H_2$ . At 2.5 K, only the normal term  $\sigma_{xy}^N$  is observed. The inset shows the itinerant spin  $\mathbf{s}$  aligned with the local moment  $\mathbf{S}_i$  on site  $i$  by a large  $J_H$ . As the electron closes the path 1-2-3-1, it acquires a Berry phase  $\phi_B$ . Panel (b) Curves of the MR  $\Delta\rho/\rho$  vs.  $H$  at selected  $T$  at 11.4 kbar (curves are offset for clarity). Below  $T_C$  (11.3 K) anomalies indicate fields  $H_1$  (uparrows),  $H_2$  (downarrows) and  $H_s$ . By comparison, the MR is nearly zero below  $H_s = 0.6$  T at ambient pressure (thin curve at 25 K).

small applied  $H$ .

Secondly,  $\sigma_{xy}^C$  is seen to be finite only within a very narrow field interval ( $H_1, H_2$ ). The relatively abrupt vanishing of  $\sigma_{xy}^C$  at  $H_2 \sim 0.45$  T is striking. Such an abrupt vanishing

of the Hall current seems impossible to realize with orbital mechanisms (carrier mobilities cannot be abruptly changed in such weak  $H$ ). By contrast, the spin-Berry phase model applied to MnSi anticipates that  $\sigma_{xy}^C$  must vanish at a field below  $H_s$ , as the cone angle of the spiral state is suppressed to zero. In the ferromagnetic state above  $H_s$ , spin textures are energetically prohibitive. As the spin textures are removed with increasing  $H$ ,  $\sigma_{xy}^C$  must vanish. Hence  $H_s$  represents an upper bound for a finite  $\sigma_{xy}^C$ . The Hall results show that the vanishing actually occurs at the slightly lower field  $H_2$ . The observed mesa profile of  $\sigma_{xy}^C(H)$  has been reproduced in a recent calculation [21] based on the bcc1 “spin-crystal” ground state of MnSi.

Thirdly, the picture described also clarifies the origin of the kink anomalies long known in MnSi under pressure [25]. The low- $T$  transverse MR of MnSi is very large and negative throughout its phase diagram because of its long  $\ell$ . Under pressure, weak anomalies appear at fields  $H < H_s$ . Figure 3b compares the transverse MR measured in our sample at ambient pressure and at 11.4 kbar with  $\mathbf{H} \perp \mathbf{I}$  (applied current). First, we examine the MR curve at ambient  $P$  (lowest curve, at 25 K, with  $T_C = 30$  K). Surprisingly, the MR is almost zero below  $H_s$ . A sharp kink at  $H_s$  signals saturation of the moments, followed by a steep decrease of  $\rho$  at larger  $H$ . The absence of MR implies that, as  $\mathbf{q}$  re-orient in  $\mathbf{H}$  and the cone angle decreases [26], there is no change in the carrier scattering rate  $\Gamma$  in  $H < H_s$  [12, 25]. Consequently, the changes below  $H_s$  involve no change in magnetic disorder or the creation of spin defects at ambient  $P$ . The “rigidity” of the spiral state at ambient pressure also explains why the Hall anomaly is not observed at ambient pressure.

By contrast, at  $P = 11.4$  kbar, the MR exhibits kinks in the interval  $0 < H < H_s$ . Above  $T_C$  (11.3 K), the MR decreases smoothly. At 11 K, the 2 field scales  $H_1$  and  $H_2$  inferred from  $\sigma_{xy}$  (Fig. 3b) become apparent (up and down arrows, respectively). Their positions change only slightly with  $T$ . However, they become more sharply defined as  $T$  approaches  $T_C$  from below. Throughout the interval  $(0, H_s)$ , the visible MR anomalies imply that changes in the magnetic structure are accompanied by the production of magnetic defects and textures which increase  $\Gamma$ . Hence, in both transport channels, the onset and disappearance of  $\sigma_{xy}^C$  at 11.4 kbar at  $H_1$  and  $H_2$  are nearly coincident with the MR anomalies.

Our experiment reveals that, when a charge current flows through a region with chiral spin textures, a large Hall current appears. The spin-texture generated Hall current disappears if the textures are erased by increasing  $H$ . Because of the abruptness of its onset and



disappearance in a narrow field interval, the new Hall conductivity  $\sigma_{xy}^C$  is easily distinguished from both the conventional AHE term and Lorentz-force term. Its distinctive profile suggests that it may serve as a sensitive detector of chiral spin textures in helical magnets. We find that, in MnSi, these textures exist over a significant region of the phase diagram below the  $T_c$  curve for  $P < P_c$ .

We thank B. Binz, A. Vishwanath and M. Hermele for valuable discussions. The research at Princeton is supported by the U.S. National Science Foundation under MRSEC Grant DMR 0213706.

<sup>†</sup>*Present address of ML:* National Institute of Standards and Technology, Boulder, CO 80305.

- 
- [1] C. Pfleiderer, S. R. Julian and G. G. Lonzarich, *Nature* **414**, 427- 429 (2001).
  - [2] C. Pfleiderer *et al.*, *Nature* **427**, 227- 231 (2004).
  - [3] C. Pfleiderer, P. Böni, T Keller, U.K. Rössler and A. Rosch, *Science* **316**, 1871 (2007).
  - [4] U. K. Rössler, U. N. Bogdanov and C. Pfleiderer, *Nature* **442**, 797- 801 (2006).
  - [5] I. Fischer, N. Shah, and A. Rosch, *Phys. Rev. B* **77**, 024415 (2008).
  - [6] S. Tewari, D. Belitz and T. R. Kirkpatrick, *Phys. Rev. Lett.* **96**, 047207 (2006).
  - [7] B. Binz, A. Vishwanath, and V. Aji, *Phys. Rev. Lett.* **96**, 207202 (2006); B. Binz and A. Vishwanath, *Phys. Rev. B* **74**, 214408 (2006).
  - [8] Y. Ishikawa and M. Arai, *J. Phys. Soc. Jpn* **53** 2726-2733, (1984).
  - [9] *Spin Fluctuation in Itinerant Electron Magnetism*, T. Moriya, Springer Series in Solid-State Sciences, Springer, Berlin (1985); and references therein.
  - [10] C. Pfleiderer, G. J. McMullan, S. R. Julian and G. G. Lonzarich, *Phys. Rev. B* **55**, 8330 (1997).
  - [11] N. Manyala, *et al.* *Nature Materials* **3**, 255-262 (2004).
  - [12] M. Lee, Y. Onose, Y. Tokura and N. P. Ong, *Phys. Rev. B* **75**, 172403 (2007).
  - [13] R. Karplus and J. M. Luttinger, *Phys. Rev.* **95**, 1154 (1954).
  - [14] Ganesh Sundaram and Qian Niu, *Phys. Rev. B* **59**, 14915 (1999).
  - [15] M. Onoda, N. Nagaosa, *J. Phys. Soc. Jpn.* **71**, 19 (2002).
  - [16] T. Jungwirth, Qian Niu, A. H. MacDonald, *Phys. Rev. Lett.* **88**, 207208 (2002).

- [17] J. Ye *et al.*, Phys. Rev. Lett. **83**, 3737 (1999).
- [18] Gen Tatara and Hikaru Kawamura, Jnl. Phys. Soc. Jpn., **71**, 2613 (2002).
- [19] P. Matl *et al.*, Phys. Rev. B **57**, 10248 (1998).
- [20] Y. Taguchi, Y. Oohara, H. Yoshizawa, N. Nagaosa, Y. Tokura, Science **291**, 2573 (2001).
- [21] B. Binz and A. Vishwanath, Physica B **403**, 1336 (2008).
- [22] Y. J. Uemura *et al.*, Nature Physics **3**, 29 (2007).
- [23] W. Yu *et al.*, Phys. Rev. Lett. **92** 086403 (2005).
- [24] B. Fåk, R. A. Sadykov, J. Flouquet and G. Lapertot, J. Phys.: Cond. Matter **17** 1635-1644 (2005).
- [25] K. Kadowaki, K. Okuda and M. Date, J. Phys. Soc. Jpn. **51**, 2433 (1982).
- [26] Y. Ishikawa, G. Shirane, J. A. Tarvin and M. Kohgi, Phys. Rev. B **16**, 4956 (1977).